

# Multifunctionality and Cytotoxicity of a Layered Coordination Polymers

**Patrícia Silva,<sup>†,a</sup> Ricardo F. Mendes,<sup>†,a</sup> Carlos Fernandes,<sup>b</sup> Ana C. Gomes,<sup>a</sup>  
Duarte Ananias,<sup>a,c</sup> Fernando Remião,<sup>d</sup> Fernanda Borges,<sup>b</sup>  
Anabela A. Valente,<sup>a</sup> Filipe A. Almeida Paz<sup>\*,a</sup>**

*<sup>†</sup> Authors contributed equally to the present work*

*A contribution from*

*<sup>a</sup> Departamento de Química, CICECO – Aveiro Institute of Materials, Universidade de Aveiro, 3810-193 Aveiro, Portugal*

*<sup>b</sup> CIQUP - Centro de Investigação em Química, Departamento de Química e Bioquímica, Faculdade de Ciências, Universidade do Porto, 4169-007 Porto, Portugal*

*<sup>c</sup> Departamento de Física, CICECO – Aveiro Institute of Materials, Universidade de Aveiro, 3810-193 Aveiro, Portugal*

*<sup>d</sup> UCIBIO-REQUIMTE, Laboratório de Toxicologia, Departamento de Ciências Biológicas, Faculdade de Farmácia, Universidade do Porto, 4050-313 Porto, Portugal*

## Electronic Supporting Information

---

*\* To whom correspondence should be addressed:*

Filipe A. Almeida Paz  
Department of Chemistry, CICECO  
University of Aveiro  
3810-193 Aveiro  
Portugal

E-mail: [filipe.paz@ua.pt](mailto:filipe.paz@ua.pt)  
FAX: (+351) 234 401470  
Telephone: (+351) 234 401418

# Table of Contents

## Table of Contents

<b>1. Experimental Section</b> .....	<b>S3</b>
1.1. General Instrumentation .....	S3
1.2. Reagents .....	S4
1.3. Preparation of $[\text{Gd}_2(\text{H}_3\text{nmp})_2] \cdot x\text{H}_2\text{O}$ ( $x = 1$ to 4) .....	S4
Hydrothermal synthesis: convection heating .....	S4
Microwave-assisted hydrothermal synthesis .....	S5
One-Pot synthesis: isolation of small single crystals .....	S5
1.4. Heterogeneous Catalysis .....	S6
1.5. Photoluminescence .....	S6
1.5. Cytotoxicity Studies .....	S7
<b>2. Structural Characterization</b> .....	<b>S8</b>
2.1. X-ray Diffraction .....	S8
2.2. Solid-State NMR .....	S8
2.3. FT-IR Spectroscopy .....	S9
2.4. TEM Microscopy .....	S9
<b>3. Catalytic Studies</b> .....	<b>S10</b>
3.1. FT-IR Spectroscopy .....	S10
3.2. PXRD and SEM Studies .....	S11
<b>4. Electron Microscopy</b> .....	<b>S12</b>
4.1. EDS Mapping of $[\text{Eu}_2(\text{H}_3\text{nmp})_2] \cdot x\text{H}_2\text{O}$ ( $x = 1$ to 4) .....	S12
4.2. EDS Mapping of $[(\text{Gd}_{0.95}\text{Eu}_{0.05})_2(\text{H}_3\text{nmp})_2] \cdot x\text{H}_2\text{O}$ ( $x = 1$ to 4) .....	S13
<b>5. Photoluminescence Studies</b> .....	<b>S14</b>
<b>References</b> .....	<b>S15</b>

# 1. Experimental Section

## 1.1. General Instrumentation

Scanning Electron Microscopy (SEM) images were collected using a high resolution scanning electron microscope equipped with a Schottky emission gun Hitachi SU-70 (4 kV) with a working distance of about 10 mm. Some samples were also analysed using a Hitachi S-4100 field emission gun tungsten filament instrument working at 25 kV and with a working distance of about 15 mm. All materials have been prepared by deposition on aluminum sample holders followed by carbon coating performed on a carbon evaporator Emitech K950. SEM mapping images and STEM of  $[\text{Ln}_2(\text{H}_3\text{nmp})_2] \cdot x\text{H}_2\text{O}$  ( $x = 1$  to 4) were recorded using an Hitachi SU-70 working at 15 or 30 kV.

TEM (Transmission Electron Microscopy) images were acquired using a HR-TEM Hitachi H9000na. A suspension of  $[\text{Gd}_2(\text{H}_3\text{nmp})_2] \cdot x\text{H}_2\text{O}$  ( $x = 1$  to 4) in ethanol was sonicated for 180 seconds. One drop of this suspension was placed on a carbon-coated copper grid and left in open air to dry. TEM analysis showed that  $[\text{Gd}_2(\text{H}_3\text{nmp})_2] \cdot x\text{H}_2\text{O}$  ( $x = 1$  to 4) is extremely sensitive to the electron beam and, under normal conditions, crystallites are destroyed after a few seconds of intense irradiation. In order to minimize structural damage a minimum electron voltage was employed for the TEM measurements performed (200kV) and the magnification was kept as low as possible.

Thermogravimetric analyses (TGA) were carried out using a Shimadzu TGA 50 from ambient temperature to *ca.* 800°C, with a heating rate of 5 °C/min under a continuous stream of air with a flow rate of 20 mL/min.

Fourier Transform Infrared (FT-IR) spectra (in the spectral range 4000-400  $\text{cm}^{-1}$ ) were recorded as KBr pellets (VWR BDH Prolabo, SpectroSol, FT-IR grade; typically, 2 mg of sample were mixed in a mortar with 200 mg of KBr) using a Mattson 7000 galaxy series spectrometer equipped with a DTGS CsI detector, or using a Bruker Tensor 27 spectrometer by averaging 256 scans at a maximum resolution of 2  $\text{cm}^{-1}$ .

Routine powder X-ray diffraction (PXRD) data for all prepared materials were collected at ambient temperature on a X'Pert MPD Philips diffractometer (Cu  $\text{K}_{\alpha 1,2}$  X-radiation,  $\lambda_1 = 1.540598 \text{ \AA}$ ;  $\lambda_2 = 1.544426 \text{ \AA}$ ), equipped with an X'Celerator detector and a flat-plate sample holder in a Bragg-Brentano para-focusing optics configuration (45 kV, 40 mA). Intensity data were collected by the step-counting method (step 0.04°), in continuous mode, in the *ca.*  $5 \leq 2\theta \leq 50^\circ$  range. Variable-temperature powder X-ray diffraction data were collected on the same instrument using a high-temperature Antoon Parr HKL 16 chamber controlled by a Antoon Parr 100 TCU unit. For the present study, intensity data were collected in the step mode (0.01°, 1s per step) in the range *ca.*  $5 \leq 2\theta \leq 35^\circ$ . Data were collected between 30 °C and 740 °C.

$^{31}\text{P}$  MAS spectra were recorded at 9.4 T on a Bruker Avance 400 wide-bore spectrometer (DSX model) on a 4 mm magic-angle spinning VTN probe at 161.9 MHz.  $^{31}\text{P}$  HPDEC spectra were acquired using a 90° single pulse excitation of 3.0  $\mu\text{s}$ ; recycle delay: 60 s;  $\nu_R = 12 \text{ kHz}$ . Chemical shifts are quoted in parts per million (ppm) with respect to an 85%  $\text{H}_3\text{PO}_4$  solution.

## 1.2. Reagents

Chemicals were readily available from commercial sources and were used as received without further purification. For all tested synthetic methods, gadolinium (III) chloride hydrate (at least 99% of purity, Sigma-Aldrich) has been used as the metallic precursor in the optimization of the reaction parameters. Other lanthanide (III) chloride hydrates were used for the typical hydrothermal synthesis [ $\text{LnCl}_3 \cdot x\text{H}_2\text{O}$ ,  $\text{Ln}^{3+} = \text{Y}^{3+}$ ,  $\text{La}^{3+}$ ,  $\text{Ce}^{3+}$ ,  $\text{Pr}^{3+}$ ,  $\text{Nd}^{3+}$ ,  $\text{Sm}^{3+}$ ,  $\text{Eu}^{3+}$ ,  $\text{Tb}^{3+}$ ,  $\text{Dy}^{3+}$ ,  $\text{Ho}^{3+}$ ,  $\text{Er}^{3+}$  and  $\text{Yb}^{3+}$ ; at least 99% of purity, Sigma-Aldrich]; lanthanide (III) oxides were used for the microwave-assisted and one-pot synthesis ( $\text{Ln}^{3+} = \text{Y}^{3+}$  and  $\text{La}^{3+}$ , at least 99.99%, Inframat Advanced materials;  $\text{Ln}^{3+} = \text{Gd}^{3+}$ , at least 99.99%, Jinan Henghua Sci. & Tec. Co. Ltd). Nitrilotris(methylenephosphonic acid) [ $\text{H}_6\text{nmp}$ ,  $\text{N}(\text{CH}_2\text{PO}_3\text{H}_2)_3$ , 97%, Fluka]; hydrochloric acid (HCl, 37% Analytical Reagent Grade, Fisher Chemical); methanol (99%, Sigma-Aldrich), 1,2-epoxyhexane (97%, Sigma-Aldrich); styrene oxide ( $\geq 97\%$ , Fluka). Nonessential amino acids (NEAA), heat inactivated bovine serum (FBS), 0.25 % trypsin/1 mM EDTA, antibiotic (10,000 U/mL penicillin, 10,000  $\mu\text{g}/\text{mL}$  streptomycin), Hank's balanced salt solution without calcium and magnesium [HBSS (-/-)] were purchased from Gibco Laboratories (Lenexa, KS, USA). DMEM with high glucose, RPMI-1640 medium, 3-(4,5-dimethylthiazol-2-yl)-2,5-diphenyltetrazolium bromide (MTT), neutral red dye (NR) were acquired from Sigma-Aldrich.

## 1.3. Preparation of $[\text{Gd}_2(\text{H}_3\text{nmp})_2] \cdot x\text{H}_2\text{O}$ ( $x = 1$ to 4)

### *Hydrothermal synthesis: convection heating*

A suspension containing  $\text{H}_6\text{nmp}$  (0.153 g, 0.512 mmol) and  $\text{GdCl}_3 \cdot 6\text{H}_2\text{O}$  (0.190 g, 0.512 mmol) in *ca.* 15.0 mL of distilled water (molar ratios of about 1 : 1 : 650) was stirred thoroughly in open air (at ambient temperature) for five minutes. The resulting homogeneous suspension was transferred to an adapted Teflon-lined Parr Instruments reaction vessel (autoclave with internal volume of *ca.* 24 mL), which was then placed inside a custom preheated oven. Typically, reactions took place in a static configuration. After reacting, the vessels were allowed to cool: (i) slowly to ambient temperature or (ii) drastically under cold water (*i.e.*, autoclave quenching). *Please note:* regardless of the procedure, the isolated product was later shown to be the same by a number of characterization techniques. The contents of the autoclaves were formed by a white suspension, with the final product being recovered by vacuum filtration, washed with copious amounts of distilled water, air-dried and its crystal structure investigated using standard powder X-ray diffraction.

The synthesis conditions to prepare  $[\text{Gd}_2(\text{H}_3\text{nmp})_2] \cdot \text{H}_2\text{O}$  (**1Gd**) ( $x = 1$  to 4) were further investigated by varying the temperature (between 80 and 190 °C), the reaction time (between 1 h and 7 days), the composition of the reactive mixtures (molar ratios metal : ligand : water of about 1 : 1 : 350, 1 : 1 : 450, 1 : 1 : 550 and 1 : 1 : 650), the metal centers and metal precursor, the reactive mixture (using water as the only solvent or a mixture with volume ratio of HCl 6M/ $\text{H}_2\text{O}$  of about 1/9 or 1/1) and apparatus configuration (static or dynamic<sup>1</sup> hydrothermal conditions of the vessel).

Static hydrothermal optimal reaction conditions to obtain phase-pure **1** using  $\text{GdCl}_3 \cdot 6\text{H}_2\text{O}$ : 140-190 °C, 18-48 h, using any of the aforementioned molar ratios for the reactive mixtures. Similar experimental conditions have been used while replacing  $\text{GdCl}_3 \cdot 6\text{H}_2\text{O}$  by other  $\text{LnCl}_3 \cdot x\text{H}_2\text{O}$ , namely  $\text{Ln}^{3+} = \text{Y}^{3+}$ ,  $\text{La}^{3+}$ ,  $\text{Ce}^{3+}$ ,  $\text{Pr}^{3+}$ ,  $\text{Nd}^{3+}$ ,  $\text{Sm}^{3+}$ ,  $\text{Eu}^{3+}$ ,  $\text{Tb}^{3+}$ ,  $\text{Dy}^{3+}$ ,  $\text{Ho}^{3+}$ ,  $\text{Er}^{3+}$  and  $\text{Yb}^{3+}$ . When lanthanide (III) chloride hydrates based on  $\text{La}^{3+}$ ,  $\text{Ce}^{3+}$ ,  $\text{Pr}^{3+}$  and  $\text{Nd}^{3+}$  were used, the known and previously reported by is  $[\text{Ln}(\text{H}_3\text{nmp})] \cdot 1.5\text{H}_2\text{O}$  material could be obtained.<sup>2</sup> When  $\text{Gd}_2\text{O}_3$  was employed, **1** was readily obtained after 24 h and 48 h reaction for static and dynamic hydrothermal synthetic, respectively. Still when using  $\text{Gd}_2\text{O}_3$  but in the presence of a solvent mixture of  $\text{HCl}/\text{H}_2\text{O}$ , the optimal results were achieved for static hydrothermal synthesis: 120 °C during 12 h, using a solvent ratio of 1/2.

### ***Microwave-assisted hydrothermal synthesis***

A reactive mixture with identical chemical composition to that described for the typical hydrothermal synthesis using convection heating was stirred thoroughly in open air for five minutes. The resulting homogeneous suspension was transferred to a 10 mL IntelliVent reactor that was placed inside a CEM Focused Microwave™ Synthesis System Discover S-Class equipment. Reactions took place with constant magnetic stirring (controlled by the microwave equipment) and by monitoring the temperature and pressure inside the vessels. A constant flow of air (*ca.* 10 bar of pressure) ensured a close control of the temperature inside the vessel. After reacting, a white suspension was obtained, and the final product was recovered by vacuum filtration, followed by washing with copious amounts of distilled water, and then air-dried overnight.

The synthesis conditions to prepare  $[\text{Gd}_2(\text{H}_3\text{nmp})_2] \cdot x\text{H}_2\text{O}$  (**1Gd**) ( $x = 1$  to 4) were further investigated by varying the temperature (between 80 and 165 °C), the reaction time (between 30 seconds and 30 minutes) and the metal precursor. Optimal reaction conditions to obtain phase-pure **1Gd** when using  $\text{GdCl}_3 \cdot 6\text{H}_2\text{O}$ : molar ratio metal: ligand: water of about 1: 1: 650, temperature range 100-120 °C, 100 W of irradiation power and 10 min of reaction. The use of  $\text{Gd}_2\text{O}_3$  as the metallic precursor showed that this reactant could not be completely consumed for some reaction conditions: in most of the tests amorphous phases or mixtures of **1Gd** with the metallic precursor were typically observed.

### ***One-Pot synthesis: isolation of small single crystals***

A gel containing  $\text{H}_6\text{nmp}$  (0.1505 g, 0.503 mmol) and  $\text{Gd}_2\text{O}_3$  (0.1506 g, 0.195 mmol) in *ca.* 10.0 mL of  $\text{HCl}$  6M/ $\text{H}_2\text{O}$  was prepared in a round bottom flask and heated to reflux. The synthetic conditions used to prepare  $[\text{Gd}_2(\text{H}_3\text{nmp})_2] \cdot x\text{H}_2\text{O}$  (**1Gd**) ( $x = 1$  to 4) were investigated by systematically varying the temperature (between 100 and 120°C), the reaction time (between 12 and 48 hours) and the  $\text{HCl}/\text{H}_2\text{O}$  volume ratio (between 1/9 and 1/1). After reacting, the vessels were allowed to cool slowly to ambient temperature and crystals of the final product were readily formed after *ca.* 15 min. One-pot optimal reaction conditions to obtain phase-pure **1Gd** using  $\text{Gd}_2\text{O}_3$ : 120 °C, for 48 h, using a  $\text{HCl}/\text{H}_2\text{O}$  solvent ratio of 1/1.

**Elemental composition for the as-synthesized compound [Gd<sub>2</sub>(H<sub>3</sub>nmp)<sub>2</sub>] $\cdot$ xH<sub>2</sub>O (x = 1 to 4):**

Calculated (in %) for [Gd<sub>2</sub>(H<sub>3</sub>nmp)<sub>2</sub>] $\cdot$ H<sub>2</sub>O (MW =924.57): C 7.79, H 2.18, N 3.03 (C/N = 2.6). Found, for typical hydrothermal conditions: C 7.76, H 2.17, N 2.78 (C/N = 2.8). Found, for MWAS: C 7.20, H 2.01, N 2.76 (C/N = 2.6). Found, for One-Pot synthesis: C 7.28, H 2.30, N 2.74 (C/N = 2.7).

**Thermogravimetric analysis (TGA) data (weight losses in %) and derivative thermogravimetric peaks (DTG; in italics inside the parentheses):** For typical hydrothermal conditions: 15-140 °C -4.7% (*59 °C*), 350-425 °C -1.6% (*408 °C*), 425-620°C -4.4% (*460 °C*), 620-800 °C -3.3%. For MWAS: 30-140 °C -3.9% (*61 °C*), 320-427 °C -2.2% (*411 °C*), 430-620 °C -4.2% (*455 °C*), 620-800 °C -3.9%. For one-pot conditions: 15-140 °C -4.8% (*61 °C*), 350-430 °C -1.5% (*409 °C*), 430-620 °C -4.6% (*461 °C*), 620-800 °C -3.3%.

**Selected FT-IR data (in cm<sup>-1</sup>) for the isotypical series of compound [Gd<sub>2</sub>(H<sub>3</sub>nmp)<sub>2</sub>] $\cdot$ xH<sub>2</sub>O (x = 1 to 4):**  $\nu$ (H<sub>2</sub>O)<sub>coord</sub> = 3500 *w*;  $\nu$ (N–H) = 3005 *w*,  $\nu_{\text{sym+asym}}$ (C–H) = 2845, 2777, 2747, 2660 *w*;  $\nu$ (P–OH) = 2325 *w*;  $\delta$ (H<sub>2</sub>O) = 1630 *w*;  $\delta$ (P–CH<sub>2</sub>) = 1482, 1428, 1402, 1328 *m*;  $\nu$ (P=O) = 1208, 1172 *m-vs*;  $\nu$ ((CH<sub>2</sub>)<sub>3</sub>-N) = 1120 (shoulder), 1099, 1070, 1047 *vs*;  $\nu$ (P–O) = 1005, 988, 945, 913 *m*;  $\nu$ (P–C) = 808, 753, 723 *m*. (*Please note: the assigned bands relate to the material obtained by typical hydrothermal reaction, but the spectra were found to be invariable to the method.*)

**1.4. Heterogeneous Catalysis**

A 5 mL borosilicate batch reactor equipped with a magnetic stirrer and a valve for sampling was charged with 36 mg of the heterogeneous catalyst [Gd<sub>2</sub>(H<sub>3</sub>nmp)<sub>2</sub>] $\cdot$ xH<sub>2</sub>O (**1Gd**) (x = 1 to 4), 1 mL of methanol and 0.83 mmol (0.095 mL) of styrene oxide. The reaction was carried out under atmospheric air and immersed in an external thermostated oil bath. Replicates of the catalytic experiments were made to ensure reproducibility. The evolution of the catalytic reactions was monitored using a Varian 3900 GC equipped with a capillary column (SPB-5, 20 m  $\times$  0.25 mm) and a flame ionization detector (using 1-octene as an external standard). Reaction products were identified by GC-MS (Trace GC 2000 Series (Thermo Quest CE Instruments) - DSQ II (Thermo Scientific)) using He as the carrier gas.

Leaching tests (LT) were performed by filtering the solid catalyst through a 0.20  $\mu$ m nylon GVS membrane after 1 h of reaction of styrene oxide with methanol at 55 °C. The reaction solution was left under constant magnetic stirring for additional 3 h without the solid catalyst. A comparison of the increment in conversion in the time interval between 1 and 4 h for the reactions with and without filtration of the solid [denoted  $\Delta$ LT(1-4h)] was performed so to check for a homogeneous phase catalytic contribution.

**1.5. Photoluminescence**

Photoluminescence measurements were recorded on a Fluorolog®-3 Model FL3-2T with double excitation spectrometer (Triax 320), fitted with a 1200 grooves/mm grating blazed at 330 nm, and a single

emission spectrometer (Triax 320), fitted with a 1200 grooves/mm grating blazed at 500 nm, coupled to R928 photomultiplier. Excitation spectra were corrected from 240 to 600 nm for the spectral distribution of the lamp intensity using a photodiode reference detector. Emission spectra were corrected for the spectral response of the monochromators and the detector using typical correction spectra provided by the manufacturer. Time-resolved measurements were carried out using a 1934D3 phosphorimeter coupled to the Fluorolog®-3 and a Xe-Hg flash lamp (6  $\mu$ s/pulse half width and 20-30  $\mu$ s tail) was used as excitation source. Measurements at 12 K were performed using a He closed-cycle cryostat.

## 1.5. Cytotoxicity Studies

Cell lines and culture conditions: Human hepatocellular carcinoma cell line (HepG2 cells) and human epithelial kidney cell line (HK-2 cells) were employed as *in vitro* models.

Hepatocellular HepG2 cells (ATCC, Manassas, VA, USA) were routinely cultured in 75-cm<sup>2</sup> flasks using DMEM with 4.5 g/L glucose, supplemented with 10 % heat-inactivated FBS (v/v) and 1 % penicillin/streptomycin (v/v). Cells were maintained at 37 °C in a humidified atmosphere of 95 % air/5 % CO<sub>2</sub> and used between the 107<sup>th</sup> and 111<sup>st</sup> passages, to avoid phenotypic changes. Cultures were passaged weekly by trypsinization (0.25 % trypsin). In all experiments, the cells were seeded at the density of  $1.2 \times 10^4$  cells/cm<sup>2</sup>.<sup>3</sup>

Epithelial HK-2 cells were obtained from the American Type Culture Collection (ATCC; Manassas, VA, USA). Cells were routinely cultured as described before, using RPMI-1640 medium, supplemented with 10 % heat-inactivated FBS (v/v) and 1 % penicillin/streptomycin (v/v), and used for all the experiments between the 11<sup>st</sup> and 17<sup>th</sup> passages. In all experiments, the HK-2 cells were seeded at a density of  $1.6 \times 10^4$  cells/cm<sup>2</sup>.<sup>4</sup> Both cell lines were used 24 hours after seeding.

Cell viability assays: After confluence was reached, HepG2 and HK-2 cells were exposed to different concentrations of **1Gd** (50-400  $\mu$ g/mL) in fresh appropriate cell culture medium. The cell viability was evaluated using the MTT reduction and NR uptake assays.<sup>5</sup> After 24 hours of exposure, the cell culture medium was removed, followed by the addition of fresh cell culture medium containing 0.5 mg/mL MTT or 50  $\mu$ g/mL NR. Afterwards, HepG2 and HK-2 cells were incubated for 1 and 2 h, respectively, at 37 °C in a humidified 5 % CO<sub>2</sub>-95 % air atmosphere. In the MTT assay, after the incubation period, the cell culture medium was removed, and the formed formazan crystals dissolved in 100 % DMSO. The absorbance was measured at 550 and 690 nm in a multiwell plate reader (PowerWaveX BioTek Instruments, Vermont, US). In NR uptake assay, the cell culture medium was removed and replaced by an ethanol absolute/distilled water (1:1) solution containing 5 % of acetic acid. Absorbance was measured at 540 nm in a multiwell plate reader. Results are expressed as metabolic activity percentage and NR uptake for MTT and NR assays, respectively, using untreated cells as control cells (100 % of cell viability).

## 2. Structural Characterization

### 2.1. X-ray Diffraction

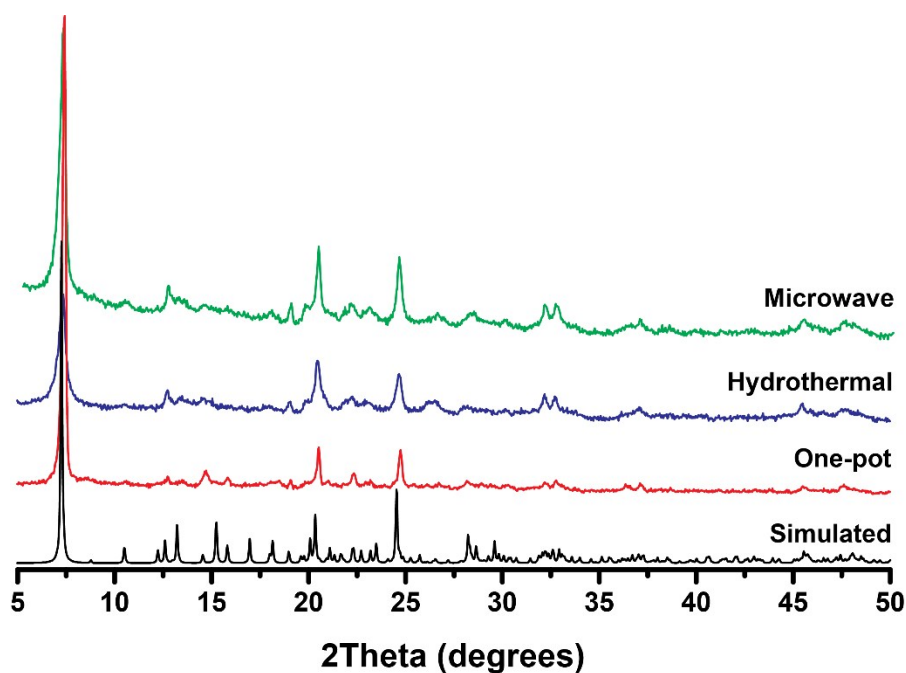


**Figure S1** – Powder X-ray diffraction of  $[\text{Gd}_2(\text{H}_3\text{nmp})_2] \cdot x\text{H}_2\text{O}$  (1Gd) obtained from the three different experimental methods reported.

### 2.2. Solid-State NMR

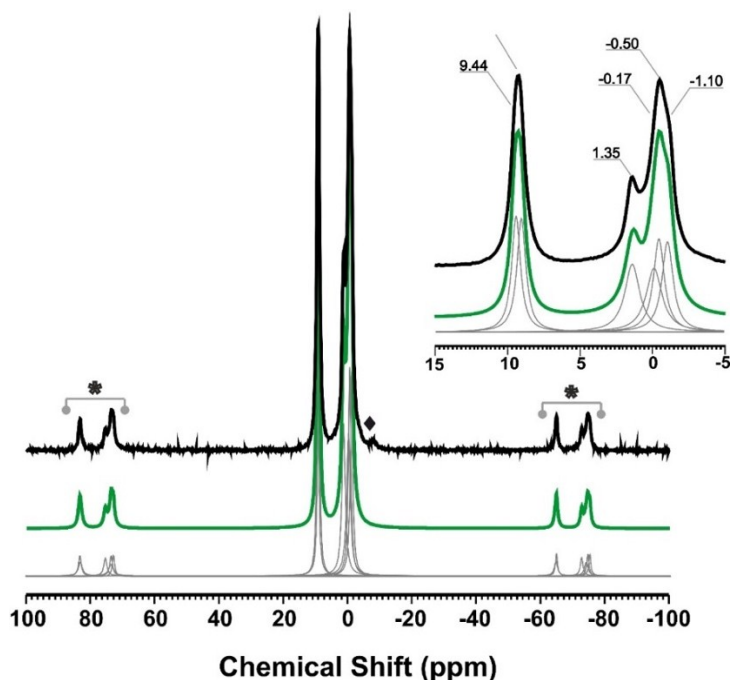
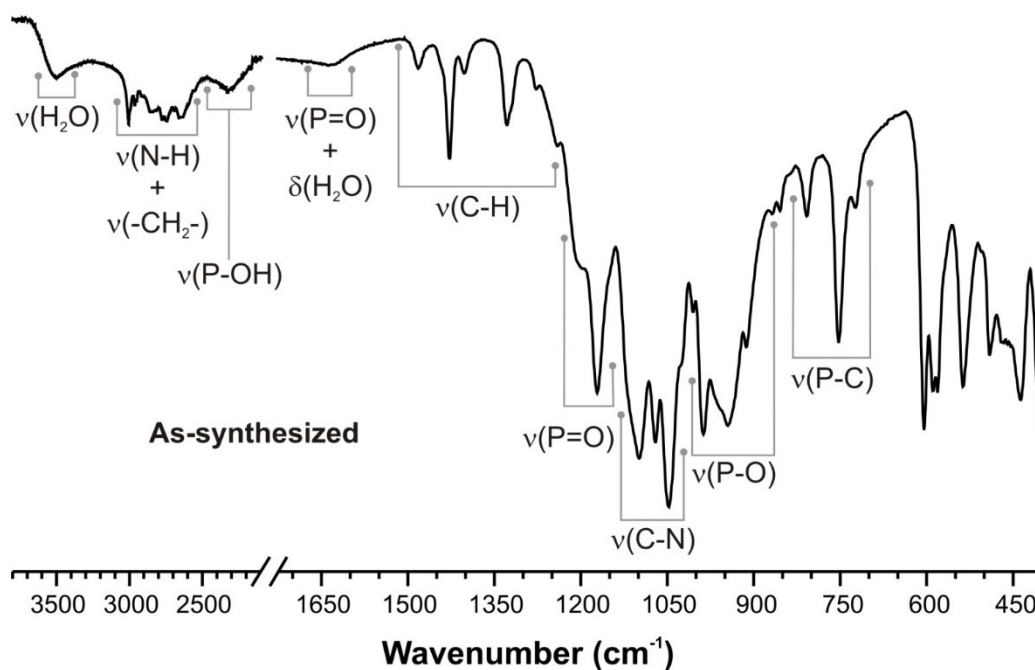


**Figure S2.**  $^{31}\text{P}$  HPDEC MAS spectrum of  $[\text{Y}_2(\text{H}_3\text{nmp})_2] \cdot x\text{H}_2\text{O}$  (1Y) ( $x = 1$  to 4). Spinning sidebands are denoted using an asterisk. Peak deconvolution and integration throughout the entire spectral range (*i.e.*, including the spinning sidebands) gives a ratio of *ca.* 1:1:1:1:1:1 for the isotropic resonances at *ca.* 9.44, 9.07, 1.35, -0.17, -0.50 and -1.10 ppm. A small impurity



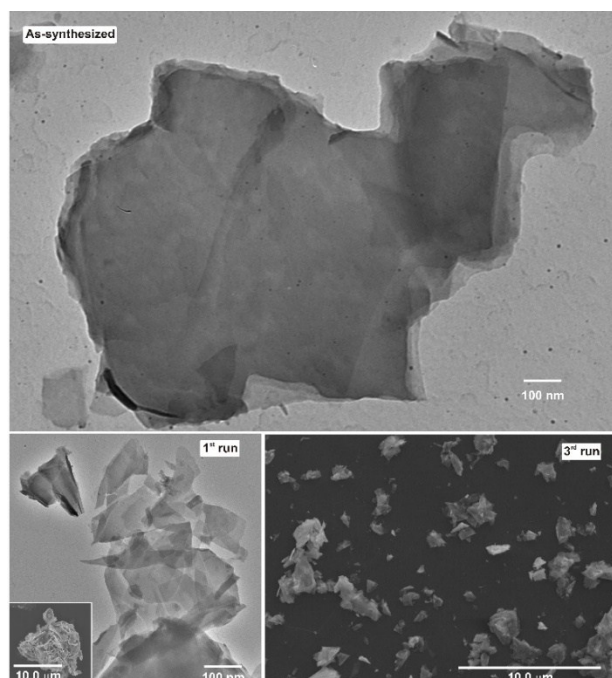
present in **1Y** is identified by a diamond symbol ( $\blacklozenge$ ). The green line represents the experimental data fit and the grey lines the fit for the single peaks.

### 2.3. FT-IR Spectroscopy



**Figure S3.** FT-IR spectra of as-synthesized  $[\text{Gd}_2(\text{H}_3\text{nmp})_2] \cdot x\text{H}_2\text{O}$  (**1Gd**) ( $x = 1$  to 4).

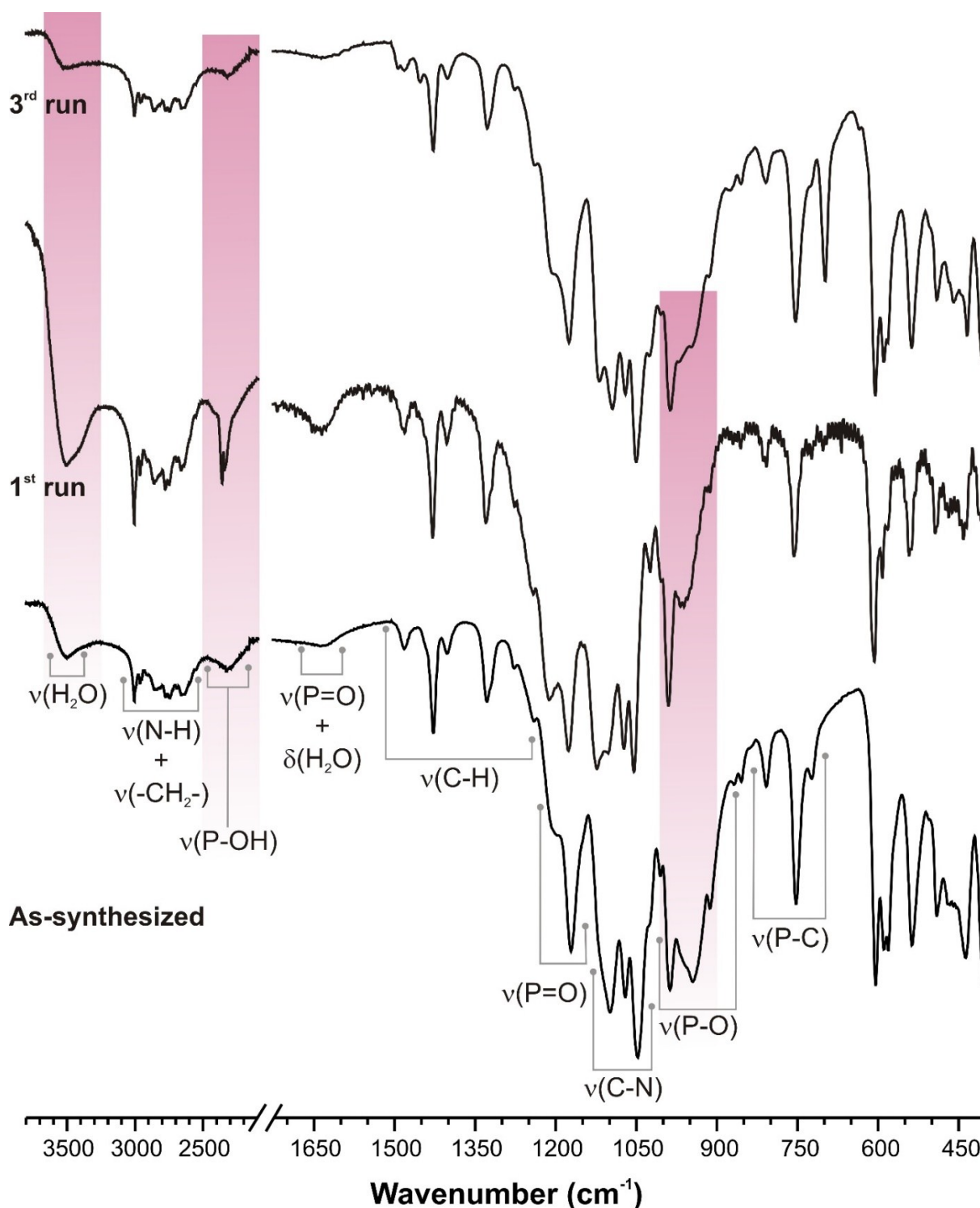
### 2.4. TEM Microscopy



**Figure S4.** TEM and SEM imaging of  $[\text{Gd}_2(\text{H}_3\text{nmp})_2] \cdot x\text{H}_2\text{O}$  (**1Gd**) ( $x = 1$  to 4) and of the solid catalyst recovered from the catalytic runs 1 and 3 (see following sections).

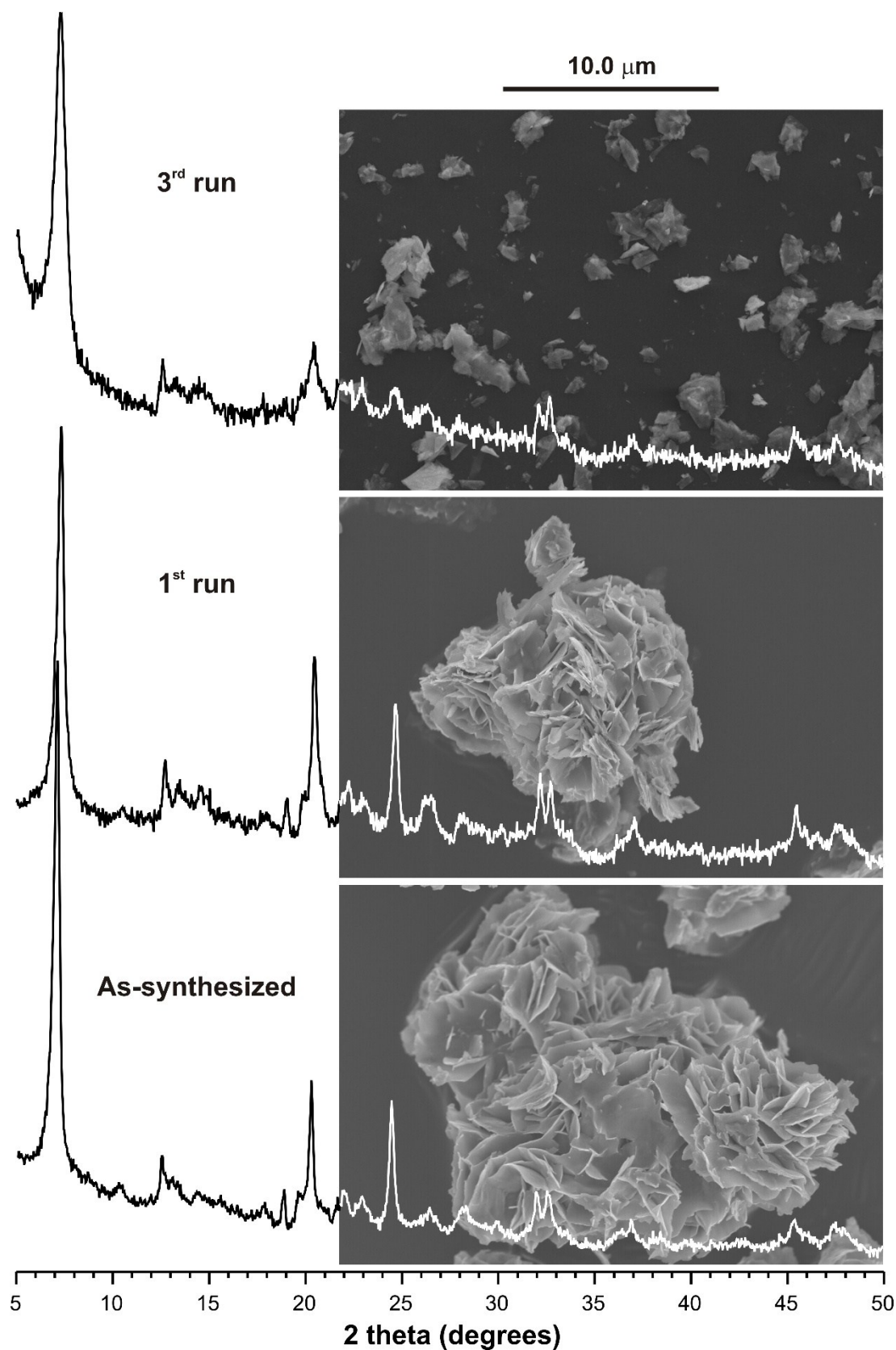
### 3. Catalytic Studies

#### 3.1. FT-IR Spectroscopy



**Figure S5.** FT-IR spectra of compound  $[\text{Gd}_2(\text{H}_3\text{nmp})_2] \cdot x\text{H}_2\text{O}$  (**1Gd**) ( $x = 1$  to  $4$ ) as-synthesized and recovered after the first and the third catalytic runs.

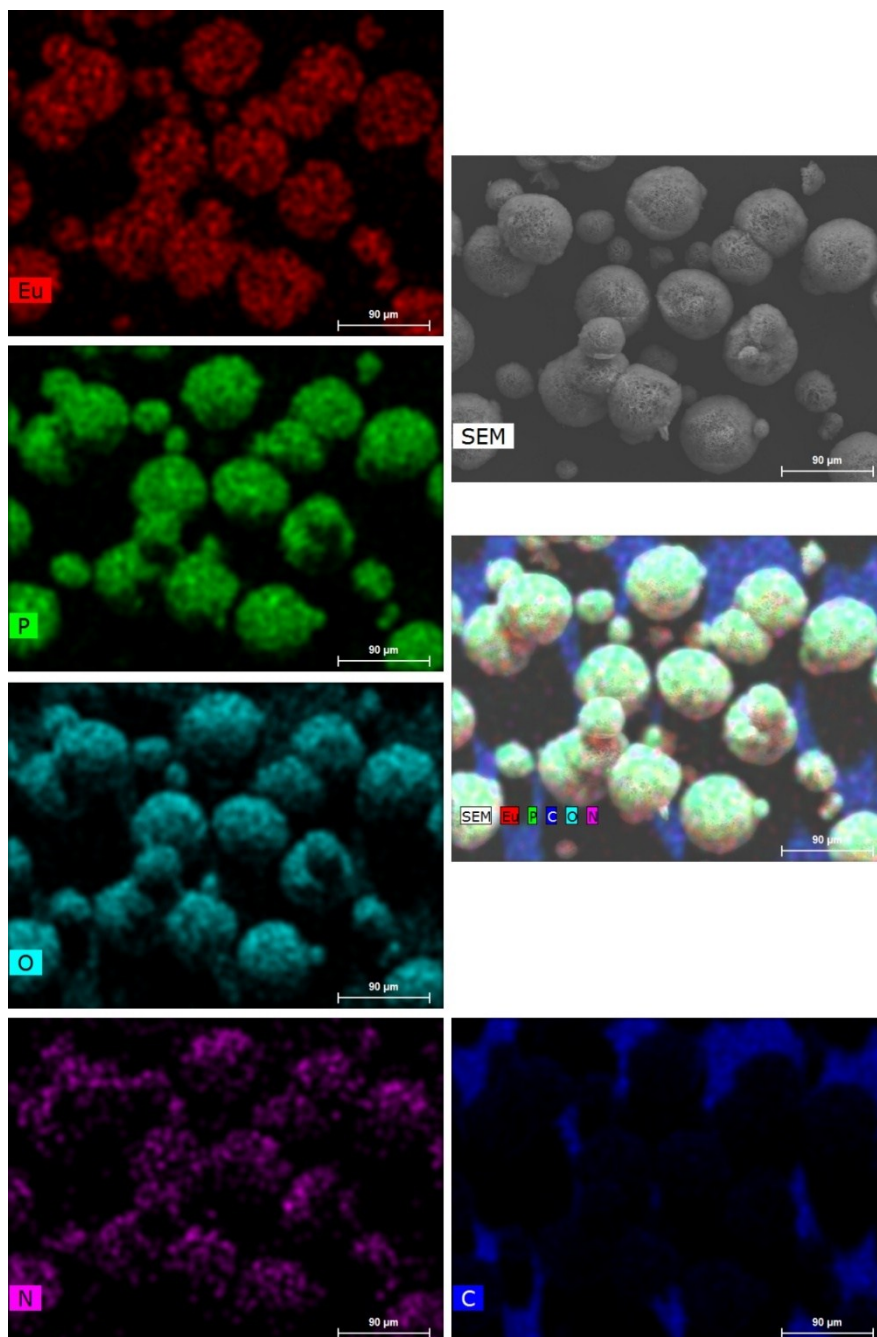
## 3.2. PXRD and SEM Studies



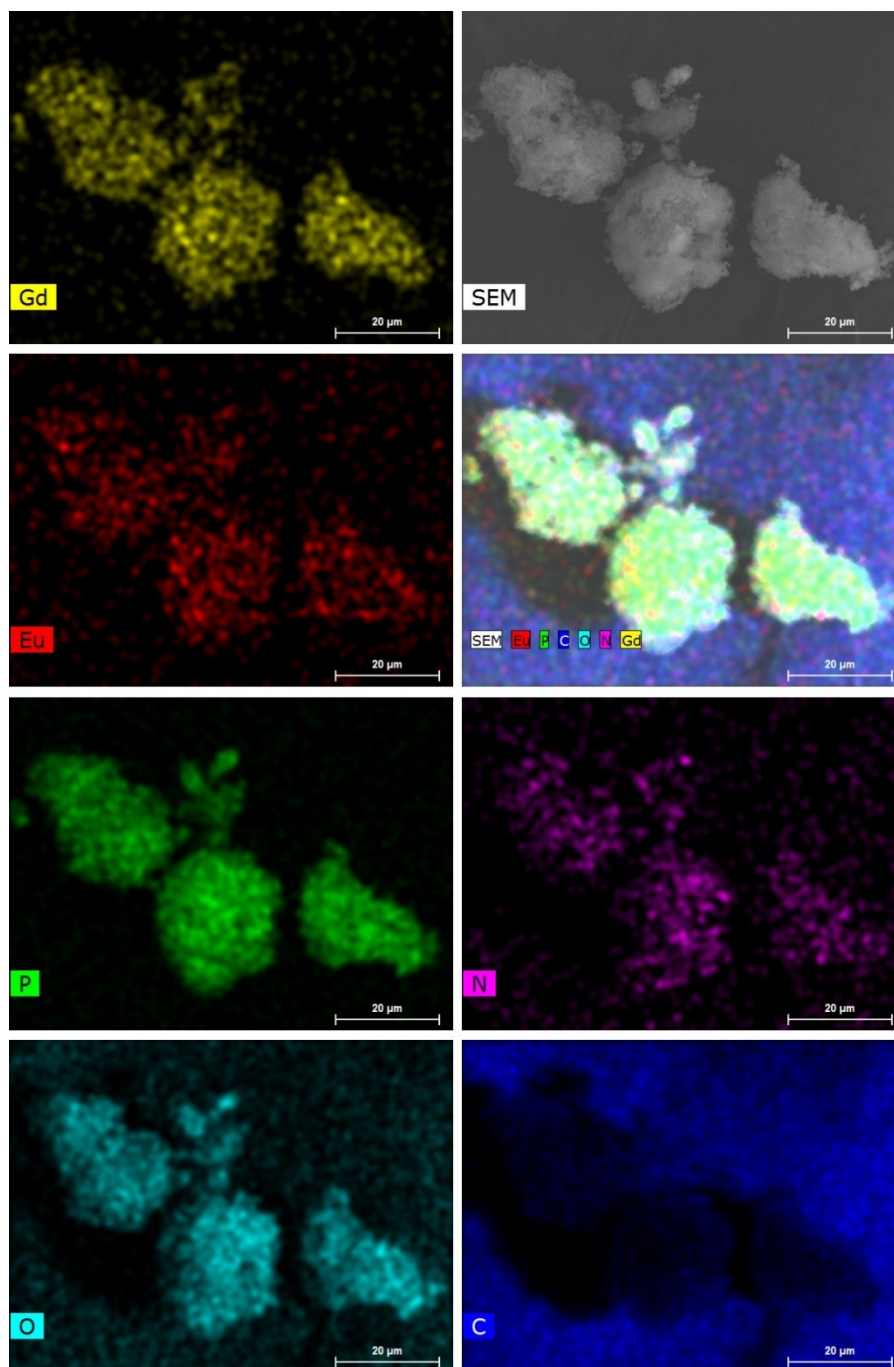
**Figure S6.** Comparison between the powder X-ray diffraction patterns and SEM images of as-synthesized  $[\text{Gd}_2(\text{H}_3\text{nmp})_2] \cdot x\text{H}_2\text{O}$  (**1Gd**) ( $x = 1$  to 4) with those of the solid catalyst recovered after runs 1 and 3.

## 4. Electron Microscopy

### 4.1. EDS Mapping of $[\text{Eu}_2(\text{H}_3\text{nmp})_2] \cdot x\text{H}_2\text{O}$ ( $x = 1$ to 4)



**Figure S7.** Electron microscopy EDS mapping studies of a portion of the  $[\text{Eu}_2(\text{H}_3\text{nmp})_2] \cdot x\text{H}_2\text{O}$  ( $x = 1$  to 4) (**1Eu**) material. Images show a uniform distribution of the heaviest elements present in the compound, thus confirming a homogeneous dispersion of both the  $\text{Eu}^{3+}$  cations and the organic ligand in the material.

**4.2. EDS Mapping of  $[(\text{Gd}_{0.95}\text{Eu}_{0.05})_2(\text{H}_3\text{nmp})_2] \cdot x\text{H}_2\text{O}$  ( $x = 1$  to 4)**

**Figure S8.** Electron microscopy EDS mapping studies of a portion of the  $[(\text{Gd}_{0.95}\text{Eu}_{0.05})_2(\text{H}_3\text{nmp})_2] \cdot x\text{H}_2\text{O}$  (**1GdEu**) ( $x = 1$  to 4) material. Images show a uniform distribution of the heaviest elements present in **1GdEu**, thus confirming a homogeneous dispersion of both the  $\text{Gd}^{3+}$  and  $\text{Eu}^{3+}$  cations, and also of the organic ligand in the material.

## 5. Photoluminescence Studies

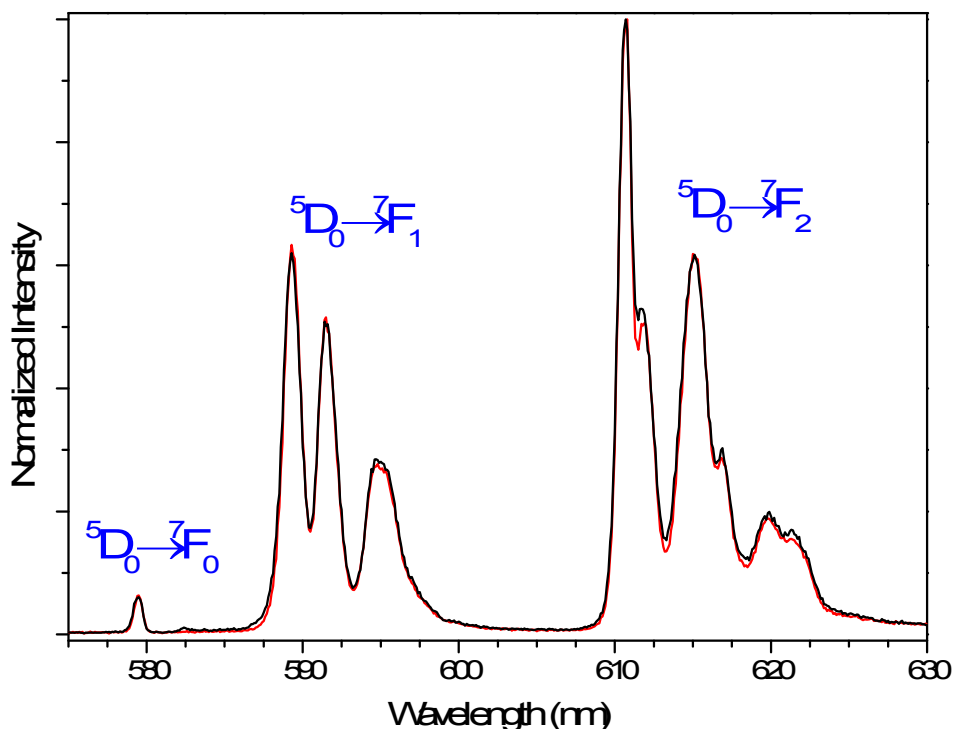


**Figure S9.** Time-resolved emission spectra of  $[\text{Eu}_2(\text{H}_3\text{nmp})_2] \cdot x\text{H}_2\text{O}$  ( $x = 1$  to  $4$ ) (**1Eu**) at 12 K with an initial delay of 0.05 ms and a sample window of 1 ms (black line), and with an initial delay of 1 ms and a sample windows of 10 ms (red line). The excitation was performed at 393 nm.

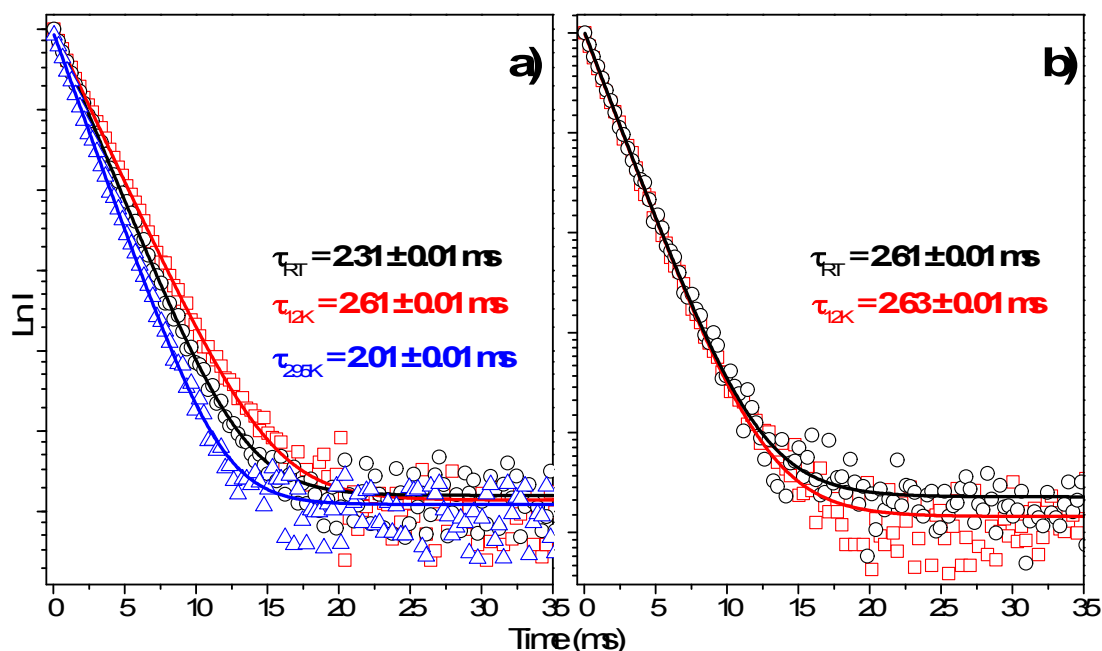


**Figure S10.**  $^5\text{D}_0$  decay curves of **(a)**  $[\text{Eu}_2(\text{H}_3\text{nmp})_2] \cdot x\text{H}_2\text{O}$  ( $x = 1$  to  $4$ ) (**1Eu**) and **(b)**  $[(\text{Gd}_{0.95}\text{Eu}_{0.05})_2(\text{H}_3\text{nmp})_2] \cdot x\text{H}_2\text{O}$  ( $x = 1$  to  $4$ ) (**1GdEu**) recorded at ambient conditions (black; temperature of 298 K and pressure of *ca.* 1 bar), at 12 K (red; pressure of *ca.*  $5 \times 10^{-6}$  mbar), and with a high vacuum (blue; temperature of 298 K and pressure of *ca.*  $5 \times 10^{-6}$  mbar). The emission was monitored at 611 nm and the excitation was performed at 393 nm. The solid lines correspond to the mathematic fits using single exponential functions.

## References

1. P. Silva, F. Vieira, A. C. Gomes, D. Ananias, J. A. Fernandes, S. M. Bruno, R. Soares, A. A. Valente, J. Rocha and F. A. A. Paz, *J. Am. Chem. Soc.*, 2011, **133**, 15120-15138.
2. L. Cunha-Silva, L. Mafra, D. Ananias, L. D. Carlos, J. Rocha and F. A. Almeida Paz, *Chem. Mat.*, 2007, **19**, 3527-3538.
3. S. Benfeito, C. Oliveira, C. Fernandes, F. Cagide, J. Teixeira, R. Amorim, J. Garrido, C. Martins, B. Sarmiento, R. Silva, F. Remião, E. Uriarte, P. J. Oliveira and F. Borges, *Eur. J. Med. Chem.*, 2019, **167**, 525-545.
4. D. Fu, S. Senouthai, J. Wang and Y. You, *Front. Immunol.*, 2019, **10**.
5. C. Fernandes, C. Martins, A. Fonseca, R. Nunes, M. J. Matos, R. Silva, J. Garrido, B. Sarmiento, F. Remião, F. J. Otero-Espinar, E. Uriarte and F. Borges, *ACS Appl. Mater. Interfaces*, 2018, **10**, 39557–39569.